Journal of Alloys and Compounds 856 (2021) 157948

Contents lists available at ScienceDirect

Journal of Alloys and Compounds

journal homepage: http://www.elsevier.com/locate/jalcom

Ni—Ti-Hf high-temperature shape memory alloy: Measure of the Clausius-Clapeyron coefficient through mechanical spectroscopy

M. Pérez-Cerrato [a, *], B. Maass [b], M.L. Nó [c], J.M. San Juan [a]

[a] Dpt. Física de la Materia Condensada, Facultad de Ciencia y Tecnología, University of the Basque Country, UPV/EHU, Apdo. 644, 48080, Bilbao, Spain
[b] Ingpuls GmbH, Von-Wadthause-Strasse 77, 44894, Bochum, Germany
[c] Dpt. Física Aplicada II, Facultad de Ciencia y Tecnología, University of the Basque Country, UPV/EHU, Apdo. 644, 48080, Bilbao, Spain

ARTICLE INFO

Article history:
Received 9 October 2020
Received in revised form
6 November 2020
Accepted 11 November 2020
Available online 21 November 2020

Keywords:
Metals and alloys
Shape memory
Mechanical properties
Phase transitions

ABSTRACT

The martensitic transformation of $Ni_{49.5}Ti_{35.5}Hf_{15}$ high temperature shape memory alloy is characterized by internal friction measurements. The temperatures for the reversible B2 ↔ B19' transformation appear in the range 410—479 K on cooling and 447—526 K on heating. In addition, a strong anomalous pre-martensitic softening of the dynamic modulus is reported in the high-temperature phase, between 850 K and 550 K, evidencing the thermoelastic character of this family of alloys. Based on the analysis of the internal friction spectra, a theoretical and experimental methodology is proposed to measure the Clausius-Clapeyron coefficient through mechanical spectroscopy. This new non-destructive method could be extremely useful for the development of advanced prototypes of shape memory alloys.

1. Introduction

The unique properties of Shape Memory Alloys (SMAs), superelasticity and shape memory, come from the microscopic mechanisms that are responsible for the reversible martensitic transformation (MT) [1,2] and are of great interest in a wide variety of applications in several technologic fields [3]. In addition, SMAs are considered as high damping materials [4] due to the motion of martensitic interfaces and there are previous works that study the way of developing high damping SMAs [5], and to this end, mechanical spectroscopy becomes a powerful tool for discovering the mechanisms responsible for the dissipation of mechanical energy [6,7]. However, the damping behaviour of SMAs is rather complex, which led to an increasing interest in understanding the processes that control this peculiar type of transformation, and looking for models that could fit the internal friction (IF) spectra of thermoelastic materials [8—11]. From the theoretical models explaining this behaviour, a lot of information can be obtained about the thermomechanical properties of the SMA, and in the present work our interest is focused on the Clausius-Clapeyron (C—C) coefficient, which in first-order phase transitions depicts the change of the transformation temperature with the applied stress. This parameter is critical in SMAs because it determines the stress-induced transformation controlling many of their applications, and usually is characterized by mechanical tests. At this point, it must be remembered that mechanical spectroscopy is a non-destructive technique and the measure of IF represents the dissipated energy per cycle and per unit of volume [12], being non-dependent on the size and shape of the sample. These aspects could become very useful when studying prototype or high-cost alloys because IF could offer the required information from only one small sample, instead of using a series of large samples. In general, this is the case of the "High Temperature Shape Memory Alloys" (HTSMA) defined as the ones with transformation temperatures above 373 K [13—16], whose development is driven by the aerospace, aeronautic and automotive industries.

Generally, the applications of SMAs are limited by their transformation temperatures, which strongly depend on the alloy composition [1—3,17—20]. Such is the case of the binary Ni—Ti, being the most successful commercially used SMA, where the transformation temperature has an upper limit of 373 K [19]. Consequently, there has been a significant number of works on the development of other binary HTSMAs, such as Ti-Pd and Ti—Pt [21,22], with Pd and Pt as substitutes of Ni. However, although the results show a huge increase on the transformation temperatures of the alloys, there is a mayor inconvenience regarding the use of such scarce and costly elements in great proportions. Therefore,

* Corresponding author.
E-mail address: mikel.perez@ehu.eus (M. Pérez-Cerrato).

https://doi.org/10.1016/j.jallcom.2020.157948

there has been an approach to understand the effects that a third, and even a fourth, element would have on the binary Ni–Ti system. Frenzel et al. [20] studied the effect that other elements have on the transformation temperatures and reported how some of them could lead to the development of new HTSMAs. Specifically, by replacing part of the Ti with Zr and/or Hf the martensitic transformation takes place at higher temperatures, and Hf exhibits the strongest effect on the transformation temperatures of the system, shifting from 340 K up to 563 K, for Hf concentrations between 2 and 20% [20,23]. Even though the transformation temperature variation is higher than 200 K, it is possible to adjust the critical temperature with an accurate control of the alloy composition [20]. Furthermore, as mentioned before, the transformation temperatures of any SMA increase with the applied stress, according to the C–C equation. In what concerns the characterization of the martensitic transformation, only recently the study of the systems Ti-Ni-Hf [24,25] and Ti–Ni–Zr [26] has been approached through mechanical spectroscopy.

Therefore, the objective of the present work is, firstly, to study the internal friction spectra of the high temperature NiTiHf SMA during the martensitic phase transformation. Then, a brief description of the theoretic background of IF associated to the martensitic transformation is offered, in order to analyse the presented results, obtained by mechanical spectroscopy, as a function of the different experimental parameters. Finally, we present a new methodology to calculate the Clausius-Clapeyron coefficient, α, through the information obtained from the internal friction spectra.

2. Materials and methods

Samples of a prototype HTSMA with nominal composition of $Ni_{49.5}Ti_{35.5}Hf_{15}$ (at.%) were provided by the company Ingpuls GmbH. The alloy was prepared in an induction furnace using high purity elements inside a graphite crucible. The alloy composition was chosen on the Ti-rich side of the diagram [27] to prevent the formation of precipitates that could evolve with aging, like the frequently reported H-phase [28,29]. The ingot was hot-rolled and the plates were thermally treated at 1223 K and quenched. Samples were water-cut into small plates of 0.9 mm × 5 mm × 50 mm for the internal friction experiments. The transformation temperatures of the alloy, martensite start and finish, $M_s = 479$ K and $M_f = 410$ K, for the direct transformation, and austenite start and finish, $A_s = 447$ K and $A_f = 526$ K, for the reverse transformation, were determined from the internal friction measurements using the method described in the following section.

The structural analysis was determined by X-ray diffraction (XRD) and electron microscopy techniques. X-ray measurements were carried out on a Bruker D8 Advance Vantec diffractometer at room temperature and at 620 K in the range of 20-70° in 2θ with the incident beam radiation of the CuKα ($\lambda = 0.15418$ nm). To characterize the microstructure of the samples, a schottky scanning electron microscope (SEM), (JEOL JSM-7000F) equipped with backscattered (BSE), X-ray (EDX, Oxford) and electron backscattered diffraction (EBSD, HKL) detectors, was initially used. Then a focus ion beam (FIB), (FEI Helios 650) was used for 3D tomography through the slice and view method, and to prepare thin lamellae. Conventional bright field (BF) transmission electron microscopy (TEM) and HAADF (High Angle Angular Dark Field) in scanning-transmission electron microscopy (STEM) were carried out at 300 KV on a FEI Titan Cubed G2 60-300 KV with a Cs-objective aberration corrector (CEOS), a gun monochromator and a super-EDX detector. All this equipment is installed at the General Service of the Basque Country University (SGIKER).

Mechanical spectroscopy experiments were conducted in a sub-resonant torsion pendulum, designed to work in inert atmosphere at a temperature range between 90 K and 1150 K, and at different frequencies that can be varied between 10^{-4} and 10 Hz, as it was previously described [30]. For the present work, some parameters such as the temperature rate and the oscillation frequency were varied along the different series of measurements. The pendulum works at constant stress amplitude σ_0, which is established through the measure of the strain ε_0, which was chosen to hold the constant value of $\varepsilon_0 = 2 \times 10^{-5}$ in austenite phase at 573 K. However, the value of ε does not remain constant during the experiment, as it is directly dependant on the elastic modulus of the material. Furthermore, for the purpose of this work, not the value of the strain but the value of the constant stress amplitude σ_0 is required to fit the equations. For this reason, some calibrations were made in order to determine the real value of σ_0, and they are described in the appendix.

3. Results and discussion

3.1. Material characterization

In Fig. 1a, the results of the X-ray diffraction experiments are shown and indexed as the B19′ martensite phase at room temperature and the B2 austenite phase at high temperature. Some authors [31] have found by neutron diffraction in richer Hf alloys, that after quenching some residual austenite B2 still remains in the martensitic state. In our case, we have not found such evidence, although it could be argued that the small peak at 41° could be interpreted as a residual of the main reflexion (110) of the B2 phase. However, we believe that it should be attributed to a small reflexion (101) appearing in martensite B19′ close to the (−1,1,1) reflexion. In any case, it is so small that cannot be analysed properly and it is no relevant for the topic of the present paper. An initial characterization by SEM and microanalysis showed that at room temperature the sample is (fully) transformed to martensite and two types of precipitates were found, and although the complete microstructural characterization is out of the scope of the present work, a short description is offered. The Fig. 1b, taken in STEM-HAADF mode, shows the microstructure of B19' martensite plates and some sub-micrometer dark precipitates, for which the EDX analysis indicates that they are Ti-richer and Ni-poorer than the matrix, with constant Hf. In Fig. 1c, taken in bright field, a detail of the martensite plates is presented to illustrate the general small size of the variants, which are strongly faulted. Finally, Fig. 1d, also taken in STEM-HAADF mode, shows a view of the second kind of precipitates, appearing in the image as very small white particles (about 100 nm in diameter) surrounded by the dark precipitates described in Fig. 1b. FIB tomography shows that these small precipitates are really embedded in the bigger dark ones, and super-EDX analysis in TEM indicates that they are still richer in Hf (46% at Hf) and contain Ti and some C, being probably some complex carbides. When these small precipitates appear, the composition of the dark ones become richer in Ti and Hf, close to $(Ti+Hf)_2Ni$, approaching the stoichiometry corresponding to the Ti_2Ni precipitates in the Ti-rich side of the binary phase diagram [32].

3.2. The IF spectrum in Ni–Ti-Hf

The thermoelastic MT is a reversible first order phase transition, which takes place without long distance atomic diffusion processes, being of displacive character involving distortions and shuffles inside the crystalline lattice. As a consequence, the progress of the transformation requires an overcooling, taking place in local equilibrium at the interfaces between the thermal driving force and the elastic stresses generated for the accommodation of both lattices [33,34]. This makes that the transformation has certain

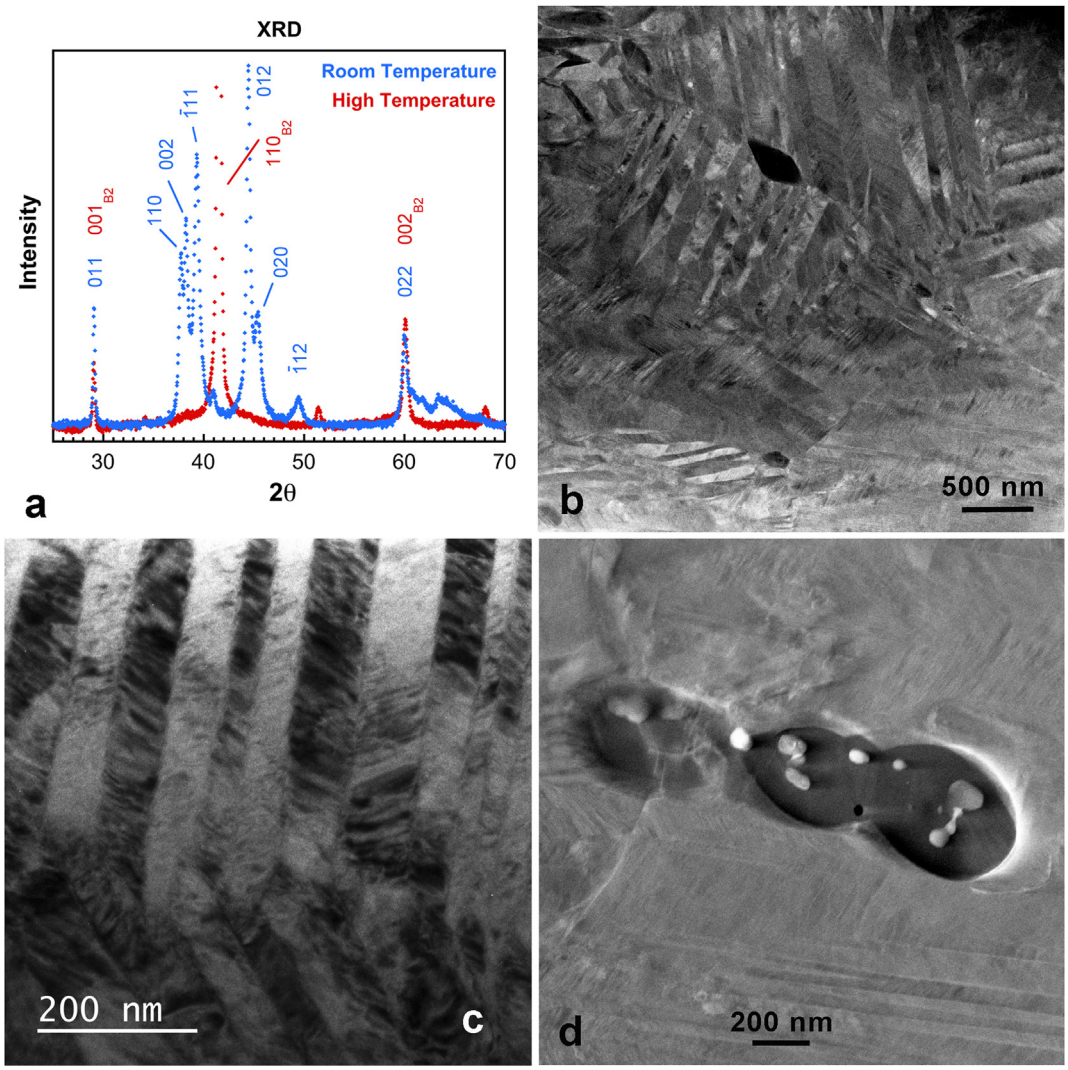

Fig. 1. (a) X-Ray Diffraction of the $Ni_{49.5}Ti_{35.5}Hf_{15}$ alloy at room temperature (blue dots) and at high temperature, 620 K (red dots). The indexation of the peaks show the B2 austenite and the B19′ martensite phases. (b) STEM-HAADF image at room temperature showing the martensite plates and black precipitates (see text). (c) TEM bright field image showing the detail of thin martensites strongly faulted. (d) Detail of Hf-rich small precipitates embedded inside the black ones similar to those of (b). (For interpretation of the references to colour in this figure legend, the reader is referred to the Web version of this article.)

temperature broadening between M_s and M_f during the direct (or forward) transformation, from austenite to martensite by cooling, and between A_s and A_f during the further reverse transformation, from martensite to austenite by heating, as well as a thermal hysteresis between the direct and reverse transformations.

Internal friction measurements give a peak associated to each one of these two transformations, and Fig. 2a shows such peaks measured in the sample of Ni–Ti-Hf HTSMA under study, where the broadening and hysteresis of the transformations is clearly evidenced. The figure also records the dynamic modulus variation during the experiment, showing a softening of the material associated to the transformation. Indeed, on one side this softening is due to the high mobility of the austenite-martensite interfaces created during the transformation, and on the other side is due to the intrinsic softening of the elastic constants of the alloy. This last aspect is well illustrated in Fig. 2b, where the anomalous softening of the dynamic modulus of the austenite extends along 300 K. This type of softening is common in SMA and in particular in several Ni–Ti alloys [35–37] but it was not yet reported in Ni–Ti-Hf HTSMA. This softening is due to the instability of the austenite in the pre-transitional state, which undergoes a strong decrease of the C' and C_{44} elastic constants, as was extensively described in the review of Otsuka and Ren [32]. In order to do a further analysis of the peaks associated to the MT, it is recommended to measure the IF of the SMAs starting the experiment above the value of A_f. In this way the direct transformation is measured in the first place by cooling, and its corresponding reverse transformation is then measured during the further heating. This is the procedure used in the present work.

3.3. Analysis of the IF peak

Each one of the IF peaks associated to the MT, is composed of different contributions, which makes the quantitative analysis of the data rather complex. Fortunately, there has been a great effort to develop models that could fit the behaviour of thermo-elastic materials [8–11,38–41], and at present it is accepted that the internal friction spectrum during a martensitic transformation is composed of three different terms, which are illustrated in Fig. 3 and described as follows:

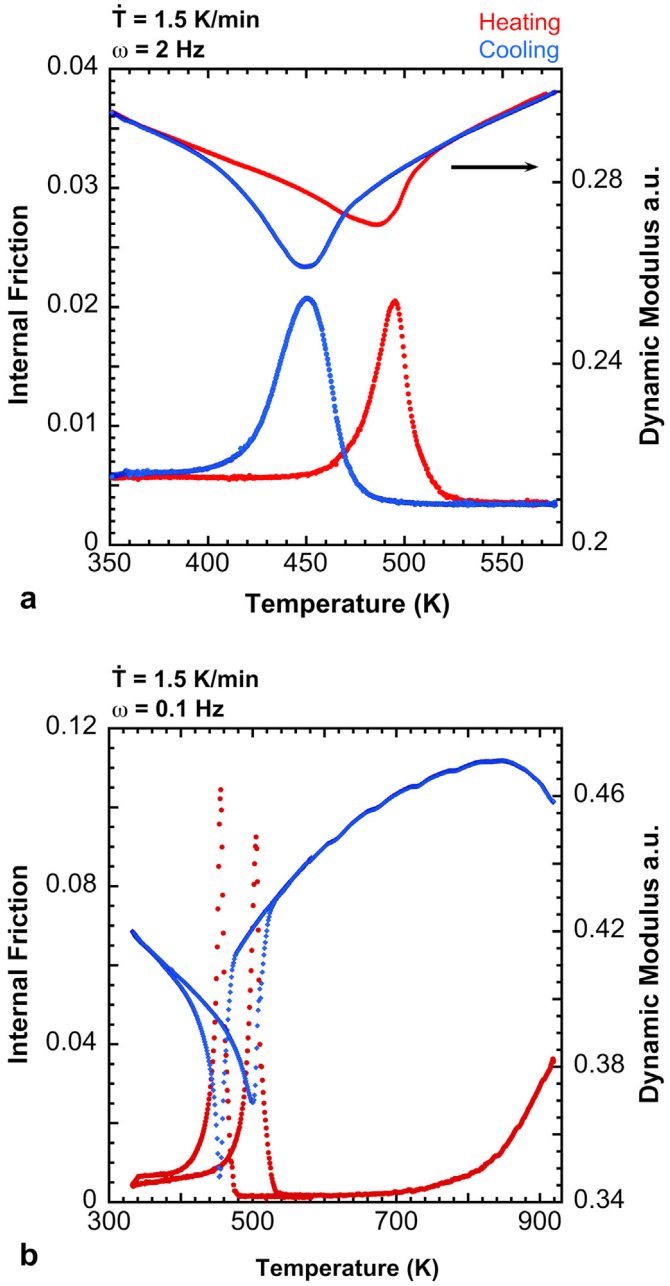

Fig. 2. IF and dynamic modulus as a function of temperature. a) The blue points depict the direct transformation of the material on cooling, and the red ones the reverse process on heating. b) Extended temperature run showing the strong softening of the dynamic modulus that extends far beyond the transformation range in the austenite phase, as the value starts dropping at about 850 K. (For interpretation of the references to colour in this figure legend, the reader is referred to the Web version of this article.)

$$IF(T) = IF_{Tr}(T) + IF_{PT}(T) + IF_{Int}(T) \quad (1)$$

The *transitory term*, $IF_{Tr}(T)$, is the kinetic part of the spectrum in IF experiments. It only appears during heating or cooling and becomes zero when measuring by steps at a constant temperature. The $IF_{Tr}(T)$ term is responsible for the strong peak that appears during the martensitic transformation and is strongly dependant on the external variables of the measurements, which include the temperature rate $\dot{T}$, the frequency of the oscillation ω and the amplitude of the applied stress σ_0. There is a general agreement on

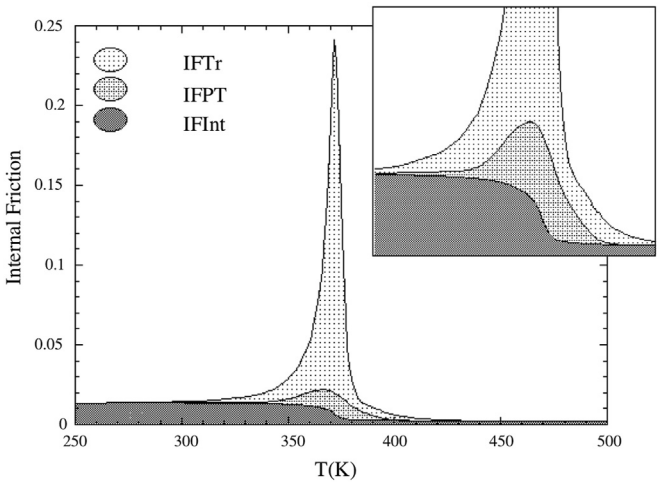

Fig. 3. Schematic representation of IF and its three contributions during a martensitic phase transformation: the transitory IF_{Tr}, the phase transformation IF_{PT} and the intrinsic IF_{Int} terms.

an expression that sums up all these different contributions, and depicts $IF_{Tr}(T)$ in a simple way [8,38]:

$$IF_{Tr}(T) = K \cdot \frac{\partial n}{\partial T} f(\dot{T}, \omega, \sigma_0) \quad (2)$$

where K is a constant, $n(T)$ is the volume fraction of transformed martensite that describes the relative amount of martensite in the material at different temperatures, so $\partial n/\partial T$, is the partial variation of the volume fraction with respect to the temperature, and $f(\dot{T}, \omega, \sigma)$ is just a general function that depends on $\dot{T}$, ω and σ_0.

The phase transformation term, $IF_{PT}(T)$, or isothermal term is associated with the transformation itself, and is the part of the peak that remains during the isothermal measurements.

Finally, the intrinsic term, $IF_{Int}(T)$, is the base contribution of each phase to the spectrum. Austenite and martensite phases have different values of the internal friction due to the difference not only of their crystal structures but also on the microstructure, which in martensite phase exhibits a pattern of self-accommodated martensite variants separated by mobile interfaces; thus $IF_{Int}(T)$ shows the relative contribution of each phase during the transformation process. There is a general agreement that the internal friction is associated to the mixture of the high and low temperature phases, with a dependence on $n(T)$ according to the following equation [8,9]:

$$IF_{Int}(T) = n(T)IF_m + [1 - n(T)]IF_a \quad (3)$$

where IF_m and IF_a are the IF contributions of the martensite and austenite respectively. Something that will be crucial for the latter analysis of the results is how to separate the different contributions, mainly $IF_{Int}(T)$, as it represents the background of the spectrum. The method described in Refs. [8,9] has been systematically used to obtain a numerical expression for $IF_{Int}(T)$. It consists of an iterative method that takes an initial function for $IF_{Int}(T)$ and with each cycle the output is compared with the previous one, until it converges. The method uses the definitions given earlier, so the values for $n(T)$ are directly the transformed mass fraction derived from the experimental data, of Fig. 2 for instance, as it is shown in Fig. 4. From there, the transformation temperatures (M_s, M_f, A_s and A_f) can be determined by the temperature value at 2 and 98% of the transformation function, $n(T)$, as it is usually done in technologic applications. For this alloy we obtain $M_s = 479$ K and $M_f = 410$ K for

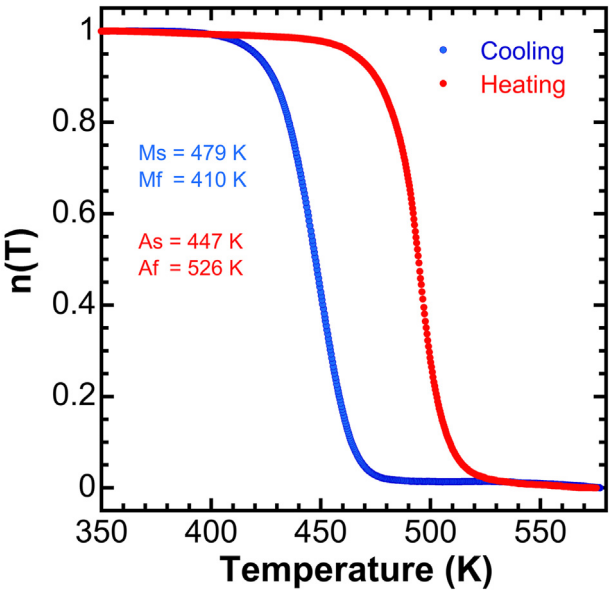

Fig. 4. Transformed volume fraction of martensite as a function of temperature. The values of the transformation temperatures are taken at 2 and 98% of transformation.

the direct transformation, and $A_s = 447$ K and $A_f = 526$ K for the reverse transformation.

A more detailed study of the different contributions that define the thermoelastic internal friction spectra can be found in Ref. [11]. The separation of the other two terms can be neglected, as the intensity of $IF_{Tr}(T)$ is much bigger than $IF_{PT}(T)$ and can be proven that those terms are only comparable at high frequencies or in isothermal conditions [8,9,11]. By subtracting $IF_{\mathrm{Int}}(T)$ to the spectrum, one obtains the contributions directly related to the phase transformation, $IF_{Tr}(T)$ and $IF_{PT}(T)$, but, as it was previously stated, it can be considered that: $IF_{Tr}(T) + IF_{PT}(T) \approx IF_{Tr}(T)$.

3.4. Dependence of $IF_{Tr}(T)$ on external parameters

The theoretical model that offers the best fitting of the IF during the thermoelastic MT, is the one developed by Gremaud et al. [38,41], which was successfully tested in several alloys by different authors [8–11,40,41]. This model is based on the influence of the stress on the first order phase transitions, which is tightly related to the C–C equation. This model portrays an analytical expression for the function f of equation (2), whose graphical representation can be seen in Fig. 5 and whose equations, according to the original model of Gremaud [38], are as follows:

$$IF_{Tr}(T) = \frac{2\varepsilon^t}{J}\frac{\partial n}{\partial T}\frac{1-\frac{\pi}{2\alpha}\frac{\dot{T}}{\omega\cdot\sigma_0}}{1+\frac{\pi}{2\alpha}\frac{\dot{T}}{\omega\cdot\sigma_0}}\cdot\frac{\dot{T}}{\omega\cdot\sigma_0}; \quad \frac{\dot{T}}{\omega\cdot\sigma_0} < \frac{2\alpha}{3\pi} \tag{4a}$$

$$IF_{Tr}(T) = \frac{\varepsilon^t}{4J}\frac{\partial n}{\partial T}\left(\frac{\dot{T}}{\omega\cdot\sigma_0}+\frac{2\alpha}{\pi}\right); \quad \frac{2\alpha}{3\pi} < \frac{\dot{T}}{\omega\cdot\sigma_0} < \frac{2\alpha}{\pi} \tag{4b}$$

$$IF_{Tr}(T) = \frac{\varepsilon^t}{2J}\frac{\partial n}{\partial T}\frac{\dot{T}}{\omega\cdot\sigma_0}; \quad \frac{2\alpha}{\pi} < \frac{\dot{T}}{\omega\cdot\sigma_0} \tag{4c}$$

where ε^t is the crystallographic strain associated to the shape change of the transformation, J is the elastic compliance and α is the stress induced change of critical temperature defined as the variation of the critical temperature T_t per unit of applied stress $\alpha = dT_t/d\sigma$, (this α is not directly the one corresponding to the slope of the C–C equation, but it's inverse value). Here, we have to note that the approximation of considering $IF_{Tr}(T) + IF_{PT}(T) \approx IF_{Tr}(T)$, remains good except eventually for the values of $\dot{T}/\omega \approx 0$, this means very close to the origin in Fig. 5. Thus, equation (4b) can be described with the expression of a straight line as follows:

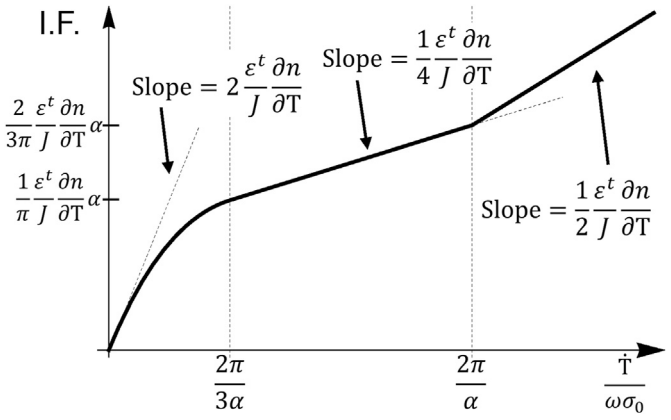

Fig. 5. Graphical representation of the Gremaud et al. model [38]. The graph shows the different regions given by equations (4a), (4b) and (4c).

$$f\left(\frac{\dot{T}}{\omega\cdot\sigma_0}\right) = \frac{\varepsilon^t}{4J}\cdot\frac{\partial n}{\partial T}\cdot\frac{1}{\sigma_0}\cdot\frac{\dot{T}}{\omega}+\frac{\varepsilon^t}{4J}\cdot\frac{\partial n}{\partial T}\cdot\frac{2\alpha}{\pi} = a\cdot\frac{\dot{T}}{\omega}+b \tag{5}$$

There is still one minor detail that has to be taken into account. According to equations (4a) to (4c), the dependence of $IF_{Tr}(T)$ is on $\dot{T}/(\omega\cdot\sigma_0)$. However, this is not a major issue, because the stress amplitude was held constant for all measurements, and although it needs to be calibrated in order to determine σ_0, the value will be constant, and equations (4a) to (4c) can be plotted as a function of just $\dot{T}/\omega$ to give a final value for the slope of the C–C equation. Then, from equation (5) the coefficient α can be obtained:

$$\alpha = \frac{\pi}{2\sigma_0}\frac{b}{a} \tag{6}$$

this expression (6) will come in handy later when the data are fitted to the models.

3.5. Measure of the Clausius-Clapeyron coefficient

The internal friction measurements were carried out using different values for the temperature rate and the oscillation frequency. The temperature rate values for heating and cooling vary from 0.5 up to 2 K/min, while oscillation frequencies were changed from 0.03 up to 4 Hz. By making different combinations between the external parameters, it is possible to obtain data that shows the dependence of the IF contributions and experimentally fit Gremaud's theoretical model. As commented above, the strain amplitude was chosen at high temperature with a value of $\varepsilon_0 = 2\times10^{-5}$ for all measurements, but was calibrated to determine the stress amplitude, which is necessary for the calculations. The calibration methodology is presented in the appendix. The dependence of the peak intensity on $\dot{T}$ and ω is shown in Fig. 6a to 6c. As it was mentioned before, all the dependence on the external parameters is carried by $IF_{Tr}(T)$, so the intrinsic term $IF_{Int}(T)$ has already been subtracted.

In addition, the high volume of measurements carried out allows showing the dependence of the height of $IF_{Tr}(T)$ on $\dot{T}$ and ω, and give a qualitative depiction of the effect that experimental

conditions have over the intensity of $IF_{Tr}(T)$, and this is illustrated in Fig. 7. The dependence shown by these results comes into agreement with the theoretical model of Gremaud, as the intensity of the transitory term is linearly dependant on the heating and cooling rates, Fig. 7a, while an increase of the frequency of oscillation decreases the intensity of the transformation peak, Fig. 7b, and also in agreement with the results reported for the Ti–Ni-20Hf [25].

The Gremaud model is composed of different regions, which are represented by different equation (4a), (4b) and (4c), as illustrated in Fig. 5. Then, we can take the maximum value for the IF transitory term, and represent it for the different values of the experimental conditions. By doing so, a more general dependence can be drawn, which is graphically represented in Fig. 8. Linear fits of some values have been made to check the quality of the results. The region given by equation (4a) can be approximated to a straight line near the origin, and the coefficient of the first-order approximation is eight times the value of the slope that describes the line of the region

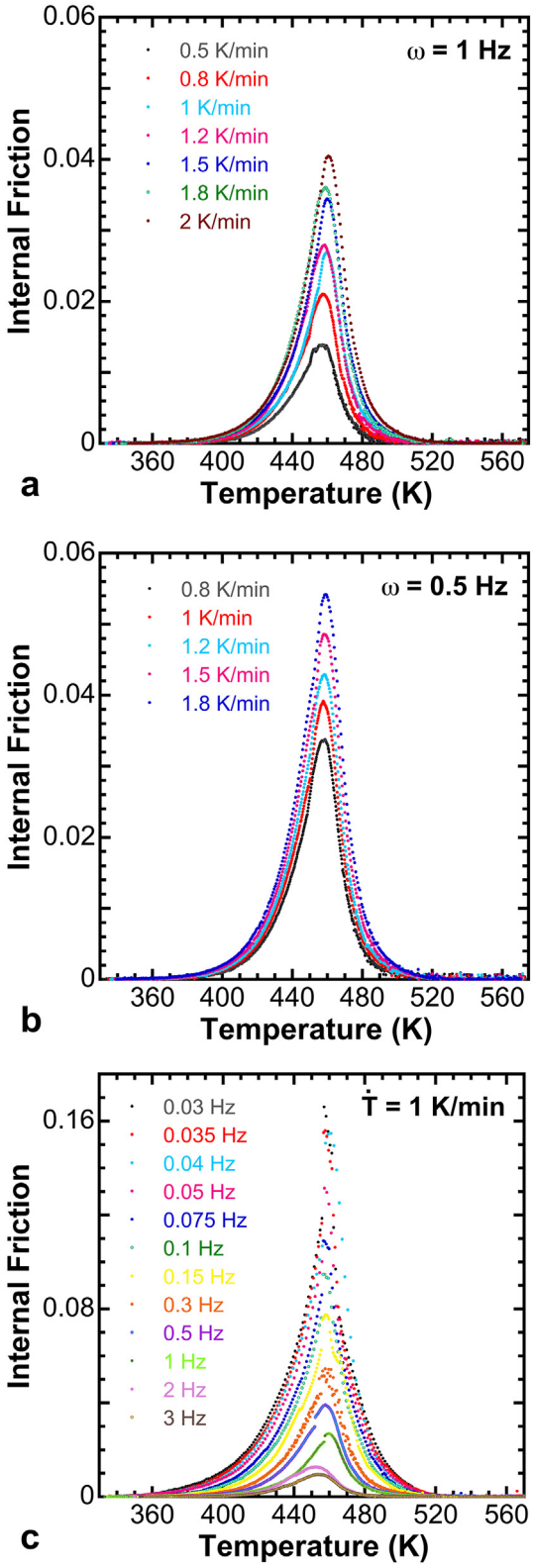

Fig. 6. The IF_{Tr} depicted for different values of the temperature rate with a constant frequency of 1 Hz (a), and 0.5 Hz (b). Plot of IF_{Tr} for different values of the oscillation frequency at a constant temperature rate of 1 K/min (c).

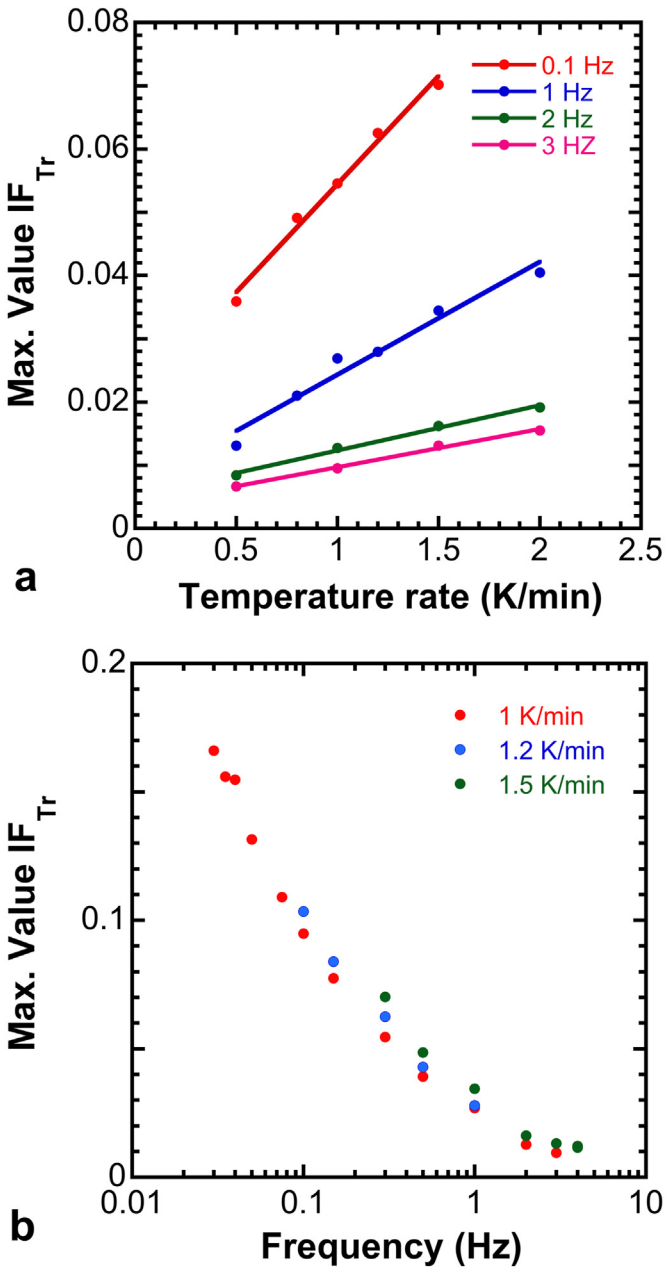

Fig. 7. Evolution of the maximum value for IF_{Tr} when measured as a function of the heating rate (a) and frequency (b) for the $Ni_{49.5}Ti_{35.5}Hf_{15}$ alloy.

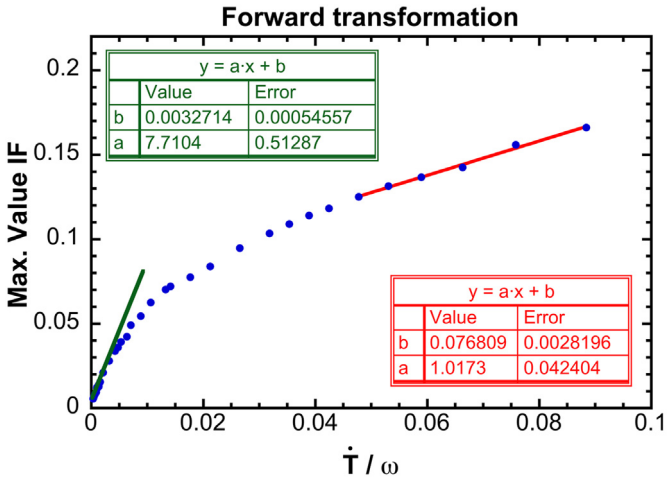

Fig. 8. Maximum value for IF_{Tr} as a function of $\dot{T}/\omega$, with the linear fits for the first and second regions performed according to Gremaud et al. model [38].

given by equation (4b). This relation is shown in Fig. 8, where the ratio between both values is $\approx$ 7.6, which is a good approximation to the theoretical value of 8. In hindsight, the only values that are needed for the calculation of the C–C coefficient are the ones included within the second region, equation (4b). Once there are enough data to properly determine the two coefficients for the linear fit, the value for C–C can be easily derived from there. In the equations, the coefficient is represented as α^{-1} (in this case α has units of K/Pa while the general representation for the C–C equation is given in Pa/K). The value of α is given by the expression (6), where a and b are the slope and the ordinate at the origin given by the linear fit of the function f in equation (5).

The value of the stress amplitude explicitly appears in the final results, so it is important to determine σ_0, which in fact only depends on the voltage applied to the magnetic coils of the pendulum. A way of measuring the relationship between the voltage V and the stress σ_0 is by means of a calibration sample, and this procedure is explained in the appendix.

Once the value for σ_0 is known the rest is simple, and in the present case of the studied $Ni_{49.5}Ti_{35.5}Hf_{15}$ sample, the imposed strain of $\varepsilon_0 = 2 \times 10^{-5}$ corresponds to a value of the stress of $\sigma_0 = 0.99$ MPa. Thus, the final value for α is given by the fitting of the experimental data, from Fig. 8, to the equation (6):

$$\alpha = \frac{\pi}{2\sigma_0}\frac{b}{a} = 0.120\,\frac{\mathrm{K}}{\mathrm{MPa}}$$

And, as the value of the C–C slope will be α^{-1}:

$$\mathrm{C-C} = (8.4 \pm 0.5)\,\frac{\mathrm{MPa}}{\mathrm{K}}$$

The value reported for this coefficient in polycrystalline binary Ni-Ti [42] ranges between 5 and 8 MPa/K. However, it has been reported that the value of the C–C coefficient becomes higher in the ternary NiTiHf alloys, and some works try to determine this coefficient in several alloys. Although the coefficient is heavily dependent on thermal treatments and crystal orientation in single crystals [43], in polycrystalline alloys the reported values for Ti–Ni-20%Hf with different microstructures [44] ranges between 7.5 and 12.5 MPa/K, and for Ti–Ni-15%Hf, values between 6.3 and 10.8 were reported [45], in rather good agreement with the value obtained in our alloy by mechanical spectroscopy. This result confirms the validity of the developed method to determine the Clausius-Clapeyron coefficient, of the SMA exhibiting thermoelastic martensitic transformations, through mechanical spectroscopy.

4. Conclusions

The thermoelastic martensitic transformation of the $Ni_{49.5}Ti_{35.5}Hf_{15}$ high temperature shape memory alloy has been characterized by mechanical spectroscopy, evidencing not only the MT peaks, but also the strong pre-martensitic softening of the high temperature austenite phase, which is also a characteristic of the thermoelastic character of the MT in this kind of alloys. The analysis of the different contributions to the internal friction transformation peak has been developed and we have shown that the $Ni_{49.5}Ti_{35.5}Hf_{15}$ alloy presents a thermoelastic behaviour that can be described through the theoretical model of Gremaud et al. [38]. From the equations describing this kind of behaviour, we propose a theoretical and experimental methodology to obtain the Clausius-Clapeyron coefficient of the alloy, from internal friction measurements. The procedure requires measuring the transformation peak at a series of points for different heating rates and frequencies, in only one sample. It will be possible to obtain the value of the Clausius-Clapeyron coefficient without the need of making superelastic tests at different temperatures and taking into account that mechanical spectroscopy is a non-destructive test, the proposed methodology will be extremely useful to characterize prototype or high-cost alloys.

CRediT authorship contribution statement

M. Pérez-Cerrato: Conceptualization, Conception and design of study, Funding acquisition, Acquisition of data, Formal analysis, Analysis and interpretation of, Data curation, data, Writing - original draft, Drafting the manuscript, Revising the manuscript critically for important intellectual content, Approval of the version of the manuscript to be published. **B. Maass:** Conceptualization, Conception and design of study, Formal analysis, Analysis and interpretation of, Data curation, data, Revising the manuscript critically for important intellectual content, Approval of the version of the manuscript to be published. **M.L. Nó:** Conceptualization, Conception and design of study, Funding acquisition, Acquisition of data, Formal analysis, Analysis and interpretation of, Data curation, data, Revising the manuscript critically for important intellectual content, Approval of the version of the manuscript to be published. **J.M. San Juan:** Conceptualization, Conception and design of study, Formal analysis, Analysis and interpretation of, Data curation, data, Writing - original draft, Drafting the manuscript, Revising the manuscript critically for important intellectual content, Approval of the version of the manuscript to be published.

Declaration of competing interest

The authors declare that they have no known competing financial interests or personal relationships that could have appeared to influence the work reported in this paper.

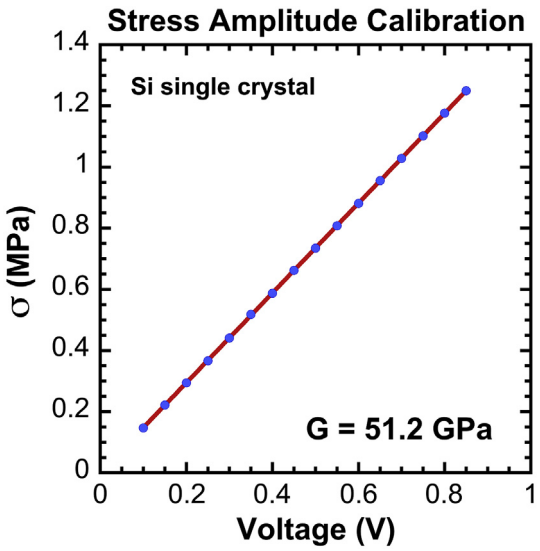

Fig. A.1. Amplitude of the applied stress vs. applied voltage in the subresonant torsion pendulum used for the IF experiments. The stress was obtained thanks to the elasticity law ($\sigma = G{\cdot}\varepsilon$), using the value of G from Ref. [47].

Acknowledgements

M. Pérez-Cerrato acknowledges the Pre-Doctoral grant (PRE_2019_2_0268) from the Education Department of the Basque Country. This work was supported by the Spanish Ministry of Economy and Competitiveness, MINECO, projects MAT2017-84069P and CONSOLIDER-INGENIO 2010 CSD2009-00013, as well as by the ELKARTEK-CEMAP project from the Industry Department of the Basque Government, and the GIU-17/071 from the UPV/EHU. This work made use of the SGIKER facilities at the University of the Basque Country.

Appendix. Calibration of the oscillation stress amplitude

For the determination of the Clausius-Clapeyron coefficient through internal friction measurements, the value for the amplitude of the applied stress is required. Generally, the mechanical spectroscopy apparatus does not give such value, as it is more common to talk about the strain amplitude during the experiment. For this reason, we have developed a procedure for the calibration of the stress amplitude applied during the internal friction experiments. Indeed, forced torsion pendulums work at constant applied stress, which only depend on the voltage V applied to the magnetic coils. It can be shown that there is a linear relationship between the voltage used and the measured strain amplitude. Using a material with a well-known shear modulus, one can measure the value of the strain ε at different values of V and then make the conversion between stress and strain via the elastic equation ($\sigma = G{\cdot}\varepsilon$) being G the value of the shear modulus of the calibration sample, as the experiment takes place just in torsion. Then, the linear relationship between V and σ_0 will be established.

In theory, any material is valid to make this type of calibration, but one must know beforehand the value of the shear modulus G of the material for one particular crystal orientation. Hence, we propose the use of a silicon wafer for the calibration. The Si wafers have the advantage of being a fairly common material, which happens to be a single crystal, and its crystal orientation is well determined (not only the normal plane to the surface, but the primary flat gives one of the directions within the plane). The values for the elastic moduli of Si have been previously measured as well [46], and more recently, Maimon et al. [47] have calculated the effective shear modulus of Si single crystal in torsional bars, giving a numerical approximation for the effective value of $G = 51.2$ GPa in a rod with [110] axial direction. We used such oriented Si single crystals and, with this value of G, obtained the different values for σ_0 for any given value of ε according to the elasticity law $\sigma = G{\cdot}\varepsilon$. Then, as shown in Fig. A.1, a linear calibration relationship between the voltage V and the amplitude of the applied stress σ_0 was established for any given material, as the value of the stress is completely independent from the sample. Finally, by measuring the voltage V required to maintain an oscillation amplitude of $\varepsilon_0 = 2 \times 10^{-5}$ in our sample of $Ni_{49.5}Ti_{35.5}Hf_{15}$ (at 573 K), we obtained the value of the stress $\sigma_0 = 0.99$ MPa reported in the text.

References

[1] K. Otsuka, C.M. Wayman (Eds.), Shape Memory Materials, Cambridge University Press, Cambridge, UK, 1998.
[2] K. Yamauchi, I. Ohkata, K. Tsuchiya, S. Miyazaki (Eds.), Shape Memory and Superelastic Alloys, Woodhead Publishing, Oxford, UK, 2011.
[3] J.M. Jani, M. Leary, A. Subic, M.A. Gibson, A review of shape memory alloy research, applications and opportunities, Mater. Des. 56 (2014) 1078–1113.
[4] N. Igata, K. Nishiyama, K. Ota, Y. Yin, W. Wuttg, I.S. Golovin, J.V. Humbeeck, J. San Juan, Panel discussion on the applications of HDM, J. Alloys Compd. 355 (2003) 230–240.
[5] J. San Juan, M.L. Nó, Damping behavior during martensitic transformation in shape memory alloys, J. Alloys Compd. 355 (2003) 65–71.
[6] G. Fantozzi, Introduction to mechanical spectroscopy: phenomenology and definitions, Mater. Sci. Forum 366–368 (2001) 3–31.
[7] J. San Juan, Mechanical spectroscopy, Mater. Sci. Forum 366–368 (2001) 32–73.
[8] R.B. Pérez-Sáez, V. Recarte, M.L. Nó, J. San Juan, Anelastic contributions and transformed volume fraction during thermoelastic martensitic transformations, Phys. Rev. B 57 (1998) 5684–5692.
[9] R.B. Pérez-Sáez, V. Recarte, M.L. Nó, J. San Juan, Analysis of the internal friction spectra during martensitic transformation by a new temperature rate method, J. Alloys Compd. 310 (2000) 334–338.
[10] J. Van Humbeeck, The martensitic transformation, Mater. Sci. Forum 366–368 (2001) 382–415.
[11] J. San Juan, R.B. Pérez-Sáez, Transitory effects, Mater. Sci. Forum 366–368 (2001) 416–437.
[12] A.S. Nowick, B.S. Berry, Anelastic Relaxation in Crystalline Solids, Academic Press, New York, USA, 1972.
[13] G.S. Firstov, J. Van Humbeeck, Y.N. Koval, High-temperature shape memory alloys: some recent developments, Mater. Sci. Eng., A 378 (2004) 2–10.
[14] J. Ma, I. Karaman, R.D. Noebe, High temperature shape memory alloys, Int. Mater. Rev. 55 (2010) 257–315.
[15] J. Van Humbeeck, Shape memory alloys with high transformation temperatures, Mater. Res. Bull. 47 (10) (2012) 2966–2968.
[16] I. López-Ferreño, J.F. Gómez-Cortés, T. Breczewski, I. Ruiz-Larrea, M.L. Nó, J.M. San Juan, High-temperature shape memory alloys based on the Cu-Al-Ni system: design and thermomechanical characterization, J. Mater. Res. Technol. 9 (2020) 9972–9984.
[17] V. Recarte, R.B. Pérez-Sáez, E.H. Bocanegra, M.L. Nó, J. San Juan, Dependence of the martensitic transformation characteristics on concentration in Cu-Al-Ni shape memory alloys, Mater. Sci. Eng., A 273–275 (1999) 380–384.
[18] X. Ren, K. Otsuka, Why does the martensitic transformation temperature strongly depend on composition? Mater. Sci. Forum 327–328 (2000) 429–432.
[19] J. Frenzel, E.P. George, A. Dlouhy, Ch Somsen, M.F.X. Wagner, G. Eggeler, Influence of Ni on martensitic transformations in NiTi shape memory alloys, Acta Mater. 58 (2010) 3444–3458.
[20] J. Frenzel, A. Wieczorek, I. Opahle, B. Maaß, R. Drautz, G. Eggeler, On the effect of alloy composition on martensite start temperatures and latent heats in Ni-Ti-based shape memory alloys, Acta Mater. 90 (2015) 213–231.
[21] K. Otsuka, K. Oda, Y. Ueno, M. Piao, The shape memory effect in a $Ti_{50}Pd_{50}$ alloy, Scripta Metall. Mater. 29 (1993) 1355–1358.
[22] T. Biggs, M. Cortie, M. Witcomb, L. Cornish, Martensitic transformations, microstructure, and mechanical workability of TiPt, Metall. Mater. Trans. 32 (2001) 1881–1886.
[23] D.R. Angst, P.E. Thoma, M.Y. Kao, The effect of hafnium content on the transformation temperatures of $Ni_{49}Ti_{51-x}Hf_x$ shape memory alloys, J. Phys. IV C8 (1995) 747–752.
[24] J. San Juan, M. Pérez-Cerrato, B. Maass, M.L. Nó, Internal friction during martensitic transformation in Ti-Ni-Hf high-temperature shape memory alloys, in: 18Th International Conference on Internal Friction and Mechanical Spectroscopy, Foz Do Iguazu, Brasil, 12-15 Sept, 2017.
[25] A. Shuitcev, L. Li, G.V. Markova, I.S. Golovin, Y.X. Tong, Internal frition in $Ti_{29.7}Ni_{50.3}Hf_{20}$ alloy with high temperature shape memory effect, Mater. Lett. 262 (2020) 127025.

[26] S. Zuo, R. Wu, G. Pang, Y. Yang, M. Jin, High temperature internal friction in $Ni_{50.3}Ti_{29.7}Zr_{20}$ shape memory alloy, Intermetallics 109 (2019) 174–178.
[27] K.P. Gupta, The Hf-Ni-Ti (Hafnium-Nickel-Titanium) system, J. Phase Equil. 22 (2001) 69–72.
[28] F. Yang, D.R. Coughlin, P.J. Phillips, L. Yang, A. Devaraj, L. Kovarik, R.D. Noebe, M.J. Mills, Structure analysis of a precipitate phase in an Ni-rich high-temperature NiTiHf shape memory alloy, Acta Mater. 61 (2013) 3335–3346.
[29] M. Prasher, D. Sen, J. Bahadur, R. Tewari, M. Krishnan, Correlative SANS and TEM investigation on precipitation kinetics of H-phase in Ni50.3Ti29.7Hf20 high temperature shape memory alloy, J. Alloys Compd. 779 (2019) 630–642.
[30] I. Gutiérrez-Urrutia, M.L. Nó, E. Carreño-Morelli, B. Guisolan, R. Schaller, J. San Juan, High performance very low frequency forced pendulum, Mater. Sci. Eng. A 370 (2004) 435–439.
[31] A. Shuitcev, R.N. Vasin, X.M. Fan, A.M. Balagurov, I.A. Bobrikov, L. Li, I.S. Golovin, Y.X. Tong, Volume effect upon martensitic transformation in Ti29.7Ni50.3Hf20 high temperature shape memory alloy, Scripta Mater. 178 (2020) 67–70.
[32] K. Otsuka, X. Ren, Physical Metallurgy of Ti-Ni based shape memory alloys, Prog. Mater. Sci. 50 (2005) 511–678.
[33] P. Wollants, J.R. Roos, L. Delaey, Thermally and stress-induced thermoelastic martensitic transformation in the reference frame of equilibrium thermodynamics, Prog. Mater. Sci. 37 (1993) 227–288.
[34] J. Rodríguez-Aseguinolaza, I. Ruiz-Larrea, M.L. Nó, A. López-Echarri, J. San Juan, A new quantitative approach to the thermoelastic martensitic transformation: the density of elastic states, Acta Mater. 56 (2008) 6283–6290.
[35] X. Ren, K. Otsuka, The role of softening in elastic constant c_{44} in martensitic transformation, Scripta Mater. 38 (1998) 1669–1675.
[36] X. Ren, N. Miura, K. Otsuka, T. Suzuki, K. Tanaki, Y.I. Chumlyakov, et al., Understanding the martensitic transformations in TiNi-based alloys by elastic constants measurement, Mater. Sci. Eng., A 273–275 (1999) 190–194.
[37] X. Ren, N. Miura, J. Zhang, K. Otsuka, K. Tanaka, M. Koiwa, et al., A comparative study of elastic constants of Ti-Ni based alloys prior to martensitic transformation, Mater. Sci. Eng. A 312 (2001) 196–206.
[38] G. Gremaud, J.E. Bidaux, W. Benoit, Etude à basse fréquence des pics de frottement intérieur associés à une transition de phase du 1er ordre, Helv. Phys. Acta 60 (1987) 947–958.
[39] J.E. Bidaux, Etude par methodes acoustiques de la transition de phase hc-cfc du cobalt, Ph.D. Thesis, EPFL, Lausanne, Switzerland, 1988. No. 761.
[40] J.E. Bidaux, R. Schaller, W. Benoit, Study of the h.c.p.-f.c.c. phase transition in cobalt by acoustic measurements, Acta Metall. 37 (1989) 803–811.
[41] J.E. Bidaux, G. Gremaud, W. Benoit, Transient internal friction and martensitic phase transformations, Mater. Sci. Forum 119–121 (1993) 299–304.
[42] Y. Liu, A. Mahmud, F. Kursawe, T. Nam, Effect of pseudoleastic cycling on the Clausius-Clapeyron relation for the stress-induced martensitic transformation in NiTi, J. Alloys Compd. 449 (2008) 82–87.
[43] S.M. Saghaian, H.E. Karaca, H. Tobe, M. Souri, R. Noebe, Y.I. Chumlyakov, Effects of aging on the shape memory behavior of Ni-rich $Ni_{50.3}Ti_{29.7}Hf_{20}$ single crystals, Acta Mater. 87 (2015) 128–141.
[44] H.E. Karaca, S.M. Saghaian, G. Ded, H. Tobe, B. Basaran, H.J. Maier, R.D. Noebe, Y.I. Chumlyakov, Effects of nanoprecipitation on the shape memory and material properties of an Ni-rich NiTiHf high temperature shape memory alloy, Acta Mater. 61 (2013) 7422–7431.
[45] A. Evirgen, I. Karaman, R. Santamarta, J. Pons, R.D. Noebe, Microstructural characterization and shape memory characteristics of the $Ni_{50.3}Ti_{34.7}Hf_{15}$ shape memory alloy, Acta Mater. 83 (2015) 48–60.
[46] J.J. Wortman, R.A. Evans, Young's modulus, Shear modulus, and Poisson's ratio in silicon and germanium, J. Appl. Phys. 36 (1965) 153–156.
[47] R. Maimon, N. Krakover, T. Tepper-Faran, Y. Gerson, S. Krylov, Simple effective shear modulus approximation for single crystal Si torsional bars, J. Micromech. Microeng. 28 (2018) 117001.